The Fourteenth International Conference on
Computational Structures Technology
23–25 August, 2022 | Montpellier, France

Proceedings of the Fourteenth International Conference on
Computational Structures Technology
Edited by B.H.V. Topping and J. Kruis
Civil-Comp Conferences, Volume 3, Paper 9.8
Civil-Comp Press, Edinburgh, United Kingdom, 2022, doi: 10.4203/ccc.3.9.8

Simple modeling of reinforced masonry arches for associated and non-associated heterogeneous limit analysis

Y. Hua and G. Milani

Department of Architecture, Built environment and Construction engineering, Technical University of Milan
Milan, Italy

Abstract

Masonry arch and vault masonry structures, one of the widespread architectural heritages in the western and eastern world, have been standing for a long era. Heterogeneous limit analysis is a powerful tool for the collapse analysis and structural safety assessment of these historical structures, which not only can predict the collapse performance of the structures in a quick manner but can consider the real discretization of the masonry most precisely. This contribution proposes a heterogeneous model for masonry arches in presence of innovative strengthening (FRP/FRCM). The reinforcement is considered suitably modifying the admissibility conditions of the constitutive law that governs the behavior of contact joints. First, the force resultants at the interface after the reinforcement is investigated. Based on that, the yield condition and flow rule in the standard heterogeneous limit analysis formulation are updated. This approach is applied to solve both associated and non-associated sliding cases. A 9-block 2D arch with FRP reinforcement is considered to show the implementation of the theory. The results of the provided example show that when analyzing the arch with reinforcement, the associated limit analysis may overestimate the ultimate load. Such overestimation will even increase when the frictional angle drops. Therefore, it is necessary to employ the non-associated flow rule for an accurate prediction of the collapse performance of reinforced arches.

Keywords: heterogeneous limit analysis; reinforcement; masonry arch; non-associated sliding

1 Introduction

Historical arch and vault masonry structures are widely diffused in the western and eastern world. Those peculiar constructions have been standing for a long era and many of them have become precious historical and monumental constructions that deserve to preserve. Thanks to the boom of computational Operational Research, heterogeneous limit analysis is becoming one of the standard tools for quickly understanding the collapse performance of those historical structures, as well as assessing their structural safety [1-5]. This powerful tool can precisely take into account the discrete nature of the masonry structures and can provide the collapse mechanism and ultimate load of the structures in a quick and reliable manner in a single step. Such analysis was first proposed by Livesley [6-7] based on the pioneering work of Heyman [8] and Kooharian [9] and now has been extended to cope with complex collapse problems by the subsequent researchers [10-15].

To include the effect of innovative strengthening techniques (e.g. FRP/FRCM) within the frame of heterogeneous limit analysis, a simple modeling approach with a minor adjustment of the governing equation of the standard limit analysis is proposed in this contribution. Recent work mostly modeled the reinforcement by introducing extra elements [16-17]. This strategy is accurate but sometimes cumbersome especially when extended to 3D problems. This work follows another thought, considering the strengthening effect by adjusting the failure surface of the contact. Many experimental and numerical studies investigated the failure mechanism of the reinforcement-brick interface and theoretically discussed the change of the failure surface after the reinforcement [18-19]. Based on these results, the formulation of the updated limit surface due to the reinforcement is first derived in the current work. The constraint regarding the constitutive law in the standard associated limit analysis is then reformed by suitably adding a spurious cohesion for each reinforced joint. Such "spurious cohesion" can be analytically calculated based on the material properties of the reinforcement. Besides, this approach is incorporated with Sequential Linear Programming (SLP) procedure [12] to solve non-associated problems with reinforcement, which is seldomly concerned in recent studies.

To illustrate the implementation of the theory, the collapse of a 9-block 2D arch with FRP reinforcement is analyzed. The effect of the reinforcement is briefly summarized and the results of the collapse employing associated and non-associated flow rules are then compared. Based on these results, the accuracy and applicability of the associated formulation are discussed.

2 Methods

To explain how to take into account the strengthening effect, we start by recalling the formulation of classic heterogeneous limit analysis, known as Lower Bound (LB) and Upper Bound (UB) theory (1)-(2), respectively. These two formulations can be easily solved through robust Linear Programming (LP) procedure and are thus popularly employed in masonry structural analysis.

$$
\begin{aligned}
&\text{maximize} && \alpha \\
&\text{subject to} && \mathbf{A}\mathbf{x} = \alpha \mathbf{f}_L + \mathbf{f}_D \\
& && \mathbf{N}\mathbf{x} - \mathbf{c}_0 = \mathbf{z} \\
& && \mathbf{z} \leqslant 0
\end{aligned} \tag{1}
$$

$$
\begin{aligned}
&\text{minimize} && -\mathbf{f}_D^T \mathbf{u} + \mathbf{c}_0^T \mathbf{p} \\
&\text{subject to} && \mathbf{f}_L^T \mathbf{u} = 1 \\
& && \mathbf{A}^T \mathbf{u} = \mathbf{q} \\
& && \mathbf{N}^T \mathbf{p} = \mathbf{q},\ \mathbf{p} \geqslant 0
\end{aligned} \tag{2}
$$

Among all the governing equations, this work especially concerns the conditions regarding the constitutive laws of the contact interfaces, i.e. yield condition and flow rule. The yield condition enforces the resultant force states at the interface containing within a limit surface (Figure 1). Any force state that reaches the limit surfaces will lead to a motion. These possible discontinuous velocities at the interface obey the flow rule. For associated sliding, the direction of the flow keeps orthogonal to the limit surface.

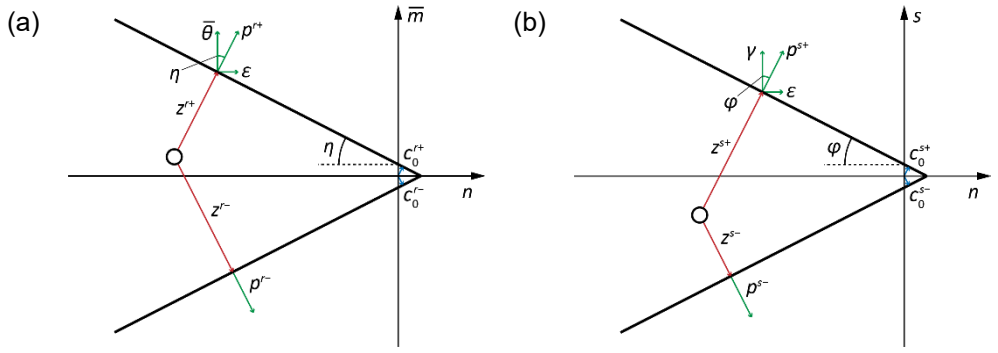

Figure 1: limit surfaces for the interface resultant forces (no reinforcement but with a small normal cohesion $\mathbf{c}_0$): (a) m-n limit surfaces; (b) s-n limit surfaces

The above limit surface will be changed due to the presence of the reinforcement. To illustrate such change, we proceed to consider all the possible forces at a representative joint with both-side strengthening (Figure 2).

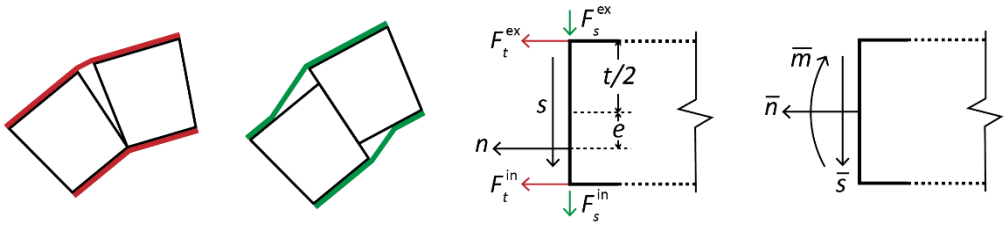

Figure 2: interface resultant forces after strengthening and equivalent description

The reinforcement produces tensive forces (F_t^{ex} and F_t^{in}) when the joint separates, while once the sliding happens, F_s^{ex} and F_s^{in} will be applied to the block because of the peeling. Taking into account these effects, the restriction of the forces at the interface then becomes:

$$
\begin{aligned}
&|e| = \left| \frac{\overline{m} - F_t^{\text{in}} \tan\eta + F_t^{\text{ex}} \tan\eta}{\overline{n} - F_t^{\text{in}} - F_t^{\text{ex}} - c_0} \right| \leqslant \tan\eta \\
&(\overline{n} - F_t^{\text{in}} - F_t^{\text{ex}} - c_0)\tan\varphi + |\overline{s}| - F_s^{\text{in}} - F_s^{\text{ex}} \leqslant 0 \\
&0 \leqslant F_t^{\text{in}} \leqslant F_{t,\max}^{\text{in}},\ \ 0 \leqslant F_t^{\text{ex}} \leqslant F_{t,\max}^{\text{ex}} \\
&0 \leqslant F_s^{\text{in}} \leqslant F_{s,\max}^{\text{in}},\ \ 0 \leqslant F_s^{\text{ex}} \leqslant F_{s,\max}^{\text{ex}}
\end{aligned} \tag{3}
$$

Constraints (3) can be shaped into a matrix form (4) that is very similar to the yield condition in (1). A spurious cohesion term $\mathbf{c}_{\text{m}}$ merely needs to be added to consider the effect of the strengthening. The components of $\mathbf{c}_{\text{m}}$ at a specific interface *j* are given in (5), which can be simply derived from the properties of the reinforced material. The LB/UB associated formulation considering the effect of reinforcement then can be updated as (6) and (7), respectively.

$$
\mathbf{N}\mathbf{x} - \mathbf{c}_0 - \mathbf{c}_m = \mathbf{z},\ \ \mathbf{z} \leqslant 0 \tag{4}
$$

$$
\mathbf{c}_{m,j} = \begin{bmatrix} c_{m,j}^{r+} \\ c_{m,j}^{r-} \\ c_{m,j}^{s+} \\ c_{m,j}^{s-} \end{bmatrix} = \begin{bmatrix} (F_{t,\max}^{\text{in}} + F_{t,\max}^{\text{ex}})\sin\varphi_j + (F_{s,\max}^{\text{in}} + F_{s,\max}^{\text{ex}})\cos\varphi_j \\ (F_{t,\max}^{\text{in}} + F_{t,\max}^{\text{ex}})\sin\varphi_j + (F_{s,\max}^{\text{in}} + F_{s,\max}^{\text{ex}})\cos\varphi_j \\ 2F_{t,\max}^{\text{in}}\sin\eta_j \\ 2F_{t,\max}^{\text{ex}}\sin\eta_j \end{bmatrix} \tag{5}
$$

$$
\begin{aligned}
\text{minimize} \quad & \alpha \\
\text{subject to} \quad & \mathbf{A}\mathbf{x} = \alpha\mathbf{f}_L + \mathbf{f}_D \\
& \mathbf{N}\mathbf{x} - \mathbf{c}_m - \mathbf{c}_0 = \mathbf{z} \\
& \mathbf{z} \leqslant 0
\end{aligned} \tag{6}
$$

$$
\begin{aligned}
\text{minimize} \quad & -\mathbf{f}_D^T\mathbf{u} + (\mathbf{c}_m^T + \mathbf{c}_0^T)\mathbf{p} \\
\text{subject to} \quad & \mathbf{f}_L^T\mathbf{u} = 1 \\
& \mathbf{A}^T\mathbf{u} = \mathbf{N}^T\mathbf{p} \\
& \mathbf{p} \geqslant 0
\end{aligned} \tag{7}
$$

Moreover, such a technique is also applicable for the non-associated case that is solved by the SLP scheme [12]. This scheme solves the non-associated problem through a sequence of associated limit analyses. We can similarly add such a cohesion $\mathbf{c}_{\text{m}}$ in the associated formulation of each iterative step to consider the strengthening effect in non-associated problems.

3 Results

To illustrate the implementation of the above formulation, the collapse of a 9-block 2D arch with both-side FRP reinforcement is studied as an example, whose dimension is shown in Figure 3. Properties of the FRP and the bricks are given in Table 1. The ultimate forces $F_{t,\max}$ and $F_{s,\max}$ are derived from the code CNR-DT200 [20] and the peel strength testing [21], respectively.

The collapse behavior of the reinforced arch is predicted by both associated and non-associated formulation, solved through LP and SLP procedures, respectively. The results are compared with those of the arch without strengthening.

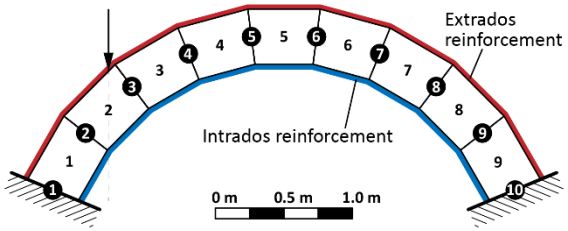

Figure 3: intrados and extrados strengthening scheme

FRP		Brick	
Thickness t_f [mm]	0.16	Width/Height/Depth [mm]	500/400/400
Young's Module E_f [GPa]	230	Compressive strength f_{bc} [MPa]	8
$F_{t,\max}$ [kN]	29.7	Tensive strength f_{bt} [MPa]	0.8
$F_{s,\max}$ [kN]	9.86	Frictional angle φ [°]	30

Table 1: several parameters for the FRP and the bricks

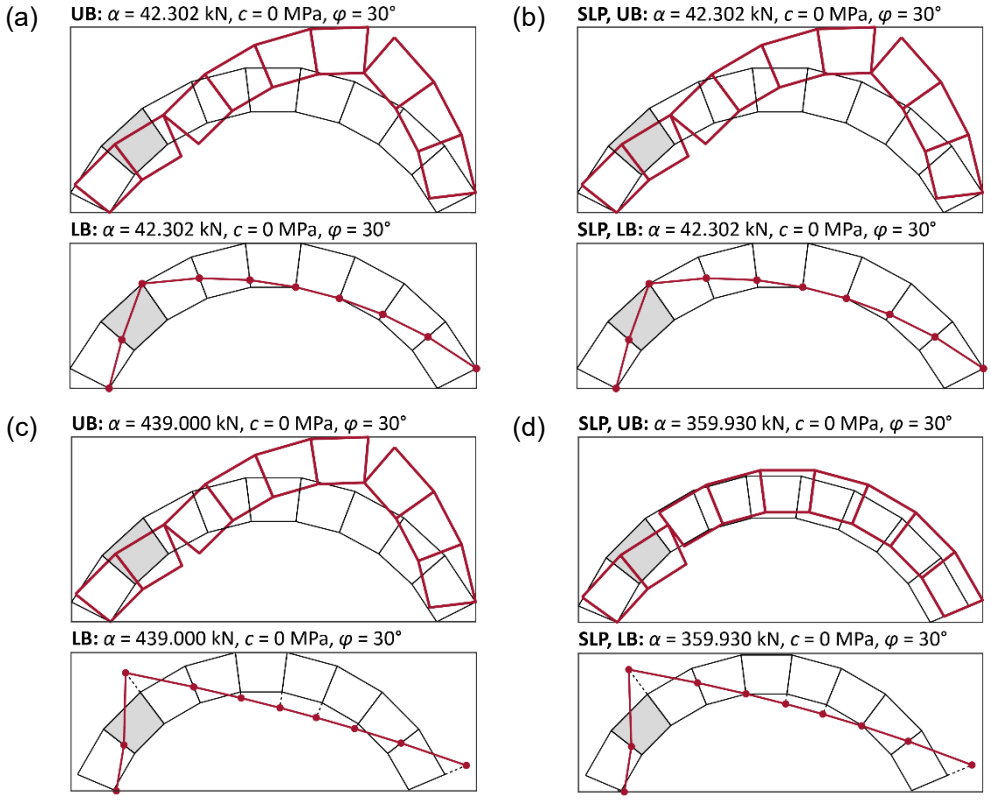

Figure 4: collapse results of the arch: (a) no reinforcement, associated flow; (b) no reinforcement, non-associated flow; (c) both-side reinforcement, associated flow; (d) both-side reinforcement, non-associated flow;

According to the result from the associated formulation, the reinforcement will not change the collapse mechanisms — all of the collapses exhibit a 4-hinge mechanism (Figure 4a and 4c). While several segments of the thrust line lay exceed the edges of the arch barrel due to the strengthening (Figure 4c). The improvement of the load

multiplier after FRP strengthening is about 937.8%. In the no-reinforcement case, the non-associated limit analysis produces consistent collapse results with those from the associated formulation (Figure 4a and 4b), while the results become different when engaging the reinforcement (Figure 4c and 4d). In-stead of a standard 4-hinge mechanism, the collapse mechanism of the non-associated analysis includes one sliding-failure joint and one sliding-rotation-mixed joint. The collapse load predicted by the associated formulation is also 21% higher than that of the non-associated one, indicating that the associated analysis could provide an overestimated result.

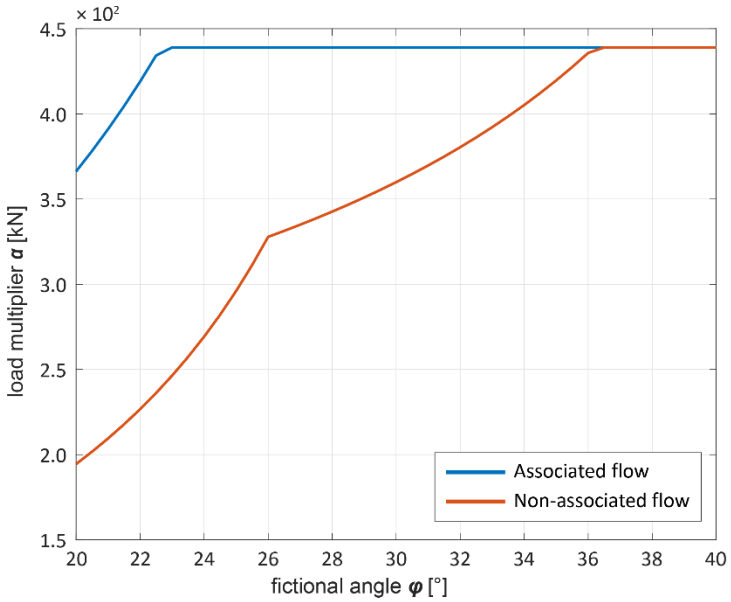

Figure 5: load multiplier vs. frictional angle: associated and non-associated flow

This contribution also investigates the influence of the frictional angle on the difference in the ultimate load (Figure 5). The curve illustrates that this difference will significantly in-crease when the frictional angle drops. Therefore, when simulating the reinforcement effect, employing the non-associated flow rule is necessary to predict an accurate collapse performance. The associated limit analysis is only recommended if the friction is high enough ($\varphi > 36°$).

4 Conclusions and Contributions

Masonry arch is a widespread structural form adopted in numerous historical buildings and infrastructures, both in the eastern and western world. Among all the numerical tools for predicting the collapse behavior of those historical structures, heterogeneous limit analysis is one of the powerful alternatives that can precisely take into account the real bond pattern of the masonry material. This contribution aims to propose a modeling strategy for including the strengthening effect within the frame of heterogeneous limit analysis, by simply updating the constraint defining the failure surface in the standard formulation. To elaborate on the implementation of this approach, the collapse analysis of a 2D arch with both-side FRP reinforcement,

employing both associated and non-associated constitutive law, is carried out as an example. The main conclusion can be drawn as follows:

- The collapse mechanism predicted by the associated formulation is the same before and after the reinforcement. While the presence of the reinforcement makes several segments of the thrust line exceed the edges of the arch barrel.
- The associated limit analysis may predict inaccurate collapse results when analyzing the arch with reinforcement: not only an overestimated ultimate load but an incorrect collapse mechanism as well. According to the result solved from the non-associated formulation, such overestimation could reach 21%, which will even increase when the frictional angle drops. Therefore, it is suggested to employ the non-associated flow rule in a general collapse analysis for a more accurate prediction. The associated limit analysis is only recommended if the friction is high enough (basically the frictional angle should be greater than 36°).
- The results of the provided example indicate that the proposed approach can take into account the effect of the strengthening to some extent. However, the accuracy of this model still needs further verification and calibration.

Acknowledgements

Yiwei Hua would like thank the financial support from China Scholarship Council (CSC) under the grant CSC No. 202108320019.

References

[1] N. Makris, H. Alexakis, The effect of stereotomy on the shape of the thrust-line and the minimum thickness of semicircular masonry arches, Arch. Appl. Mech. 83 (2013) 1511–1533. DOI: 10.1007/s00419-013-0763-4.

[2] A. Chiozzi, N. Grillanda, G. Milani, A. Tralli, UB-ALMANAC: An adaptive limit analysis NURBS-based program for the automatic assessment of partial failure mechanisms in masonry churches, Eng. Fail. Anal. 85 (2018) 201–220. DOI: 10.1016/j.engfailanal.2017.11.013.

[3] A. Chiozzi, M. Malagù, A. Tralli, A. Cazzani, ArchNURBS: NURBS-Based Tool for the Structural Safety Assessment of Masonry Arches in MATLAB, J. Comput. Civ. Eng. 30 (2016) 4015010. DOI: 10.1061/(asce)cp.1943-5487.0000481.

[4] N. Grillanda, M. Valente, G. Milani, ANUB-Aggregates: a fully automatic NURBS-based software for advanced local failure analyses of historical masonry aggregates, Bull. Earthq. Eng. 18 (2020) 3935–3961. DOI: 10.1007/s10518-020-00848-6.

[5] F.P.A. Portioli, Rigid block modelling of historic masonry structures using mathematical programming: a unified formulation for non-linear time history, static pushover and limit equilibrium analysis, Bull. Earthq. Eng. 18 (2020) 211–239. DOI: 10.1007/s10518-019-00722-0.

[6] R.K. Livesley, Limit Analysis of Structures Formed from Rigid Blocks, Int. J. Numer. Methods Eng. 12 (1978) 1853–1871.

[7] R.K. Livesley, A computational model for the limit analysis of three-dimensional masonry structures, Meccanica. 27 (1992) 161–172. DOI: 10.1007/BF00430042.

[8] J. Heyman, The stone skeleton, Int. J. Solids Struct. 2 (1966) 249–256, IN1–IN4, 257–264, IN5–IN12, 265–279. DOI: 10.1016/0020-7683(66)90018-7.

[9] A. Kooharian, Limit Analysis of Voussoir (Segmental) and Concrete Archs, ACI J. Proc. 49 (1952) 317–328. DOI: 10.14359/11822.
[10] F. Portioli, C. Casapulla, M. Gilbert, L. Cascini, Limit analysis of 3D masonry block structures with non-associative frictional joints using cone programming, Comput. Struct. 143 (2014) 108–121. DOI: 10.1016/j.compstruc.2014.07.010.
[11] M.C. Ferris, F. Tin-Loi, Limit analysis of frictional block assemblies as a mathematical program with complementarity constraints, Int. J. Mech. Sci. 43 (2001) 209–224. DOI: 10.1016/S0020-7403(99)00111-3.
[12] M. Gilbert, C. Casapulla, H.M. Ahmed, Limit analysis of masonry block structures with non-associative frictional joints using linear programming, Comput. Struct. 84 (2006) 873–887. DOI: 10.1016/j.compstruc.2006.02.005.
[13] A. Orduña, P.B. Lourenço, Three-dimensional limit analysis of rigid blocks assemblages. Part II: Load-path following solution procedure and validation, Int. J. Solids Struct. 42 (2005) 5161–5180. DOI: 10.1016/j.ijsolstr.2005.02.011.
[14] G. Milani, P.B. Lourenço, A. Tralli, Homogenised limit analysis of masonry walls, Part II: Structural examples, Comput. Struct. 84 (2006) 181–195. DOI: 10.1016/j.compstruc.2005.09.004.
[15] A. Chiozzi, G. Milani, A. Tralli, A Genetic Algorithm NURBS-based new approach for fast kinematic limit analysis of masonry vaults, Comput. Struct. 182 (2017) 187–204. DOI: 10.1016/j.compstruc.2016.11.003.
[16] A. Caporale, L. Feo, D. Hui, R. Luciano, Debonding of FRP in multi-span masonry arch structures via limit analysis, Compos. Struct. 108 (2014) 856–865. DOI: 10.1016/j.compstruct.2013.10.006.
[17] A. Caporale, L. Feo, R. Luciano, R. Penna, Numerical collapse load of multi-span masonry arch structures with FRP reinforcement, Compos. Part B Eng. 54 (2013) 71–84. DOI: 10.1016/j.compositesb.2013.04.042.
[18] G. Milani, E. Milani, A. Tralli, Upper Bound limit analysis model for FRP-reinforced masonry curved structures. Part I: Unreinforced masonry failure surfaces, Comput. Struct. 87 (2009) 1516–1533. DOI: 10.1016/j.compstruc.2009.07.007.
[19] L. Anania, G. D'Agata, Limit analysis of vaulted structures strengthened by an innovative technology in applying CFRP, Constr. Build. Mater. 145 (2017) 336–346. DOI: 10.1016/j.conbuildmat.2017.03.212.
[20] CNR-DT200, Guide for the design and construction of externally bonded FRP systems for strengthening existing structures, C.N.R., National Research Council, Italy, n.d.
[21] M. Panizza, E. Garbin, M.R. Valluzzi, Peel strength testing of FRP applied to clay bricks, in: Proc. 8th Int. Conf. Fract. Mech. Concr. Concr. Struct. Fram. 2013, 2013: pp. 562–570.